NANO LETTERS

pubs.acs.org/NanoLett Letter

Subnanometer-Precision Measurements of Transmembrane Motions of Biomolecules in Plasma Membranes Using Quenchers in Extracellular Environment

Wenqing Hou,[‖] Dongfei Ma,[‖] Xiaolong He,[‖] Weijing Han, Jianbing Ma, Hao Wang, Chunhua Xu, Ruipei Xie, Qihui Fan, Fangfu Ye, Shuxin Hu, Ming Li,* and Ying Lu*

Cite This: *Nano Lett.* 2021, 21, 485−491 Read Online

ACCESS | Metrics & More | Article Recommendations | Supporting Information

ABSTRACT: Characterization of biomolecular dynamics at cellular membranes lags far behind that in solutions because of challenges to measure transmembrane trafficking with subnanometer precision. Herein, by introducing nonfluorescent quenchers into extracellular environment of live cells, we adopted Förster resonance energy transfer from one donor to multiple quenchers to measure positional changes of biomolecules in plasma membranes. We demonstrated the method by monitoring flip-flops of individual lipids and by capturing transient states of the host defense peptide LL-37 in plasma membranes. The method was also applied to investigate the interaction of the necroptosis-associated protein MLKL with plasma membranes, showing a few distinct depths of MLKL insertion. Our method is especially powerful to quantitate the dynamics of proteins at the cytosolic leaflets of plasma membranes which are usually not accessible by conventional techniques. The method will find wide applications in the systematic analysis of fundamental cellular processes at plasma membranes.

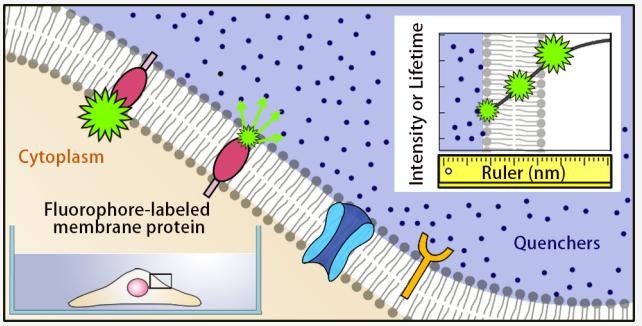

KEYWORDS: *protein−membrane interactions, live cell imaging, FRET, quenchers in extracellular environment*

Plasma membranes are permeable barriers between cells and their environment. They control the flow of information and the trafficking of substances in and out of cells and have become the target of various drugs in the process of curing diseases.[1] Many important physiological processes such as receptor−ligand interactions, lipid flip-flops, and lipid-raft formation are accompanied by the motions and structural changes of biomolecules on plasma membranes.[2,3] Current techniques such as antibody labeling and tracking and in-cell NMR have produced vast valuable findings in this field.[4−6] However, advancing the research of membrane-associated processes still demands technologies able to measure real-time positional and conformational changes of biomolecules at live-cell plasma membranes.[7] This is a substantial challenge because cellular membranes are sophisticated matrices composed of thousands of biomolecules.[8] This is especially true when positional changes in the direction normal to the membranes are the main concern.[6] One needs to extract useful information from complicated movements of the biomolecules and the membranes. Biomolecules undergo in-plane diffusions in the membranes, which in turn undergo strong out-of-plane fluctuations with amplitudes usually exceeding their thicknesses. Fluorescence imaging and spectroscopic techniques are often the methods of choice for investigating membrane proteins in live cells. Conventional Förster resonance energy transfer (FRET) can be used to measure the relative distance at the ångström scale between a pair of proteins or a pair of domains labeled with a fluorescent donor and an acceptor.[9,10] However, if the distance between a labeled protein and a cell membrane needs to be measured, it is often difficult to find a molecular component to represent the stable position in the cell membrane for fluorescent labeling.[11,12] In addition, when fluorophore-labeled molecules form clusters with unknown sizes and conformations, it is often difficult to correctly convert FRET efficiency to interfluorophore distance.[13]

We recently developed an in vitro fluorescence method to measure membrane protein dynamics in artificial lipid bilayers.[14] The method enabled us to extract information about the transmembrane motions of biomolecules while disregarding their in-plane motions. However, complex feedback networks and/or molecular crowding in cells may alter the functions and dynamics of biomolecules, potentially posing obstacles to the

Received: October 2, 2020
Revised: December 1, 2020
Published: December 5, 2020

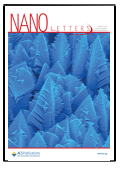

https://dx.doi.org/10.1021/acs.nanolett.0c03941
Nano Lett. 2021, 21, 485−491

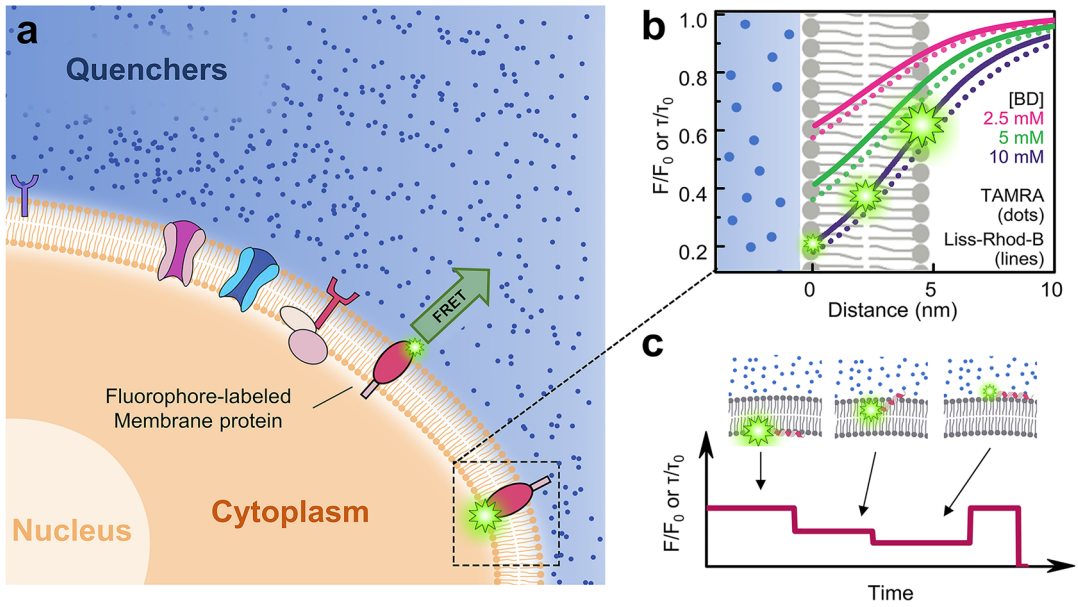

Figure 1. Principle of queenFRET. (a) Scheme of the method, in which the fluorescent energy is transferred from single fluorophores at the membrane to multiple quenchers in extracellular environment. (b) Calculated F/F_0 or τ/τ_0 vs distance at various concentrations of the quenchers. (c) Scheme of a time course of the fluorescent intensity when the fluorophore transits from the inner surface to the outer surface of a cell membrane.

physiological relevance of information gained from in vitro systems. The in vitro approach therefore cannot be directly applied to study the trafficking of biomolecules in plasma membranes of live cells. In the present work, we extend our approach to study live cells by locating quenchers in the extracellular environment during cell imaging. The feasibility of our approach relies on the appropriate selection of the quenchers. They should be neutral, water soluble, and biocompatible. Most importantly, they should not adsorb onto the cell surfaces specifically or nonspecifically. The strategy enabled us to monitor positional changes of fluorophore-labeled biomolecules relative to the plasma membrane surfaces. We anticipate that the method will significantly improve research on the dynamics of membrane proteins, responses of receptors, signal transductions across plasma membranes, and so on, which are not assessable by conventional technologies.

Design and Principle of the Method. The underlying mechanism of our method is FRET between a single fluorophore and a multitude of quenchers in extracellular environment (termed queenFRET hereafter) (Figure 1a, see details in the Supporting Information). The method does not require hardware modification to conventional fluorescence imaging microscopes. It works well with total internal reflection fluorescence microscopy (TIRF) and fluorescence lifetime imaging microscopy (FLIM). The FRET between the fluorophore and the quenchers results in a very steep change in fluorescence as the fluorophore-labeled molecule moves from the outer to the inner surface of the membrane or vice versa. The calculated FRET efficiency E as a function of the distance between the fluorophore and the quencher solution is presented in the form of relative fluorescent intensity or a relative lifetime in Figure 1b, that is, $F/F_0 = \tau/\tau_0 = 1 - E$ (see details in the Supporting Information). As a result, the positional changes of the fluorophore-labeled biomolecule in cell membranes can be reflected by its intensity or lifetime changes (Figure 1c).

In practice, one should always measure the intrinsic fluorescent intensity F_0 and the intrinsic fluorescence lifetime τ_0 of the donors in parallel with F and τ. On one hand, the measurements in the absence of the quenchers can function as a control to ensure that any changes in the fluorescent intensity are induced by the changes in the distance. On the other hand, many fluorophores may display different photophysical properties in different environments. Such environment-sensitive fluorophores should be excluded from the candidates of the donors if they display fluorescent fluctuations in the absence of the quenchers. Those that are fluorescently unstable, e.g., blinking frequently, should also be excluded. The quencher used in the present study was Blue Dextran (BD), although we believe that many other dyes with appropriate absorption spectra may be also effective. BD is a high molecular weight dextran with attached Cibacron Blue whose absorption maximum is ~600 nm[15] (see also Figure S1). BD is used in various fields such as pharmaceutical, photographic, and agricultural industries owing to its favorable properties, namely, neutrality, water solubility, and biocompatibility.[16] In our experiments, the cells remained viable even after incubation in the BD-containing culture medium overnight (Figure S2).

Flip-Flops of Lipid Molecules in Plasma Membranes. We first tested the feasibility of our method by measuring the flip-flops of fluorophore-labeled lipids. Flippases often translocate aminophospholipids, e.g., phosphatidylserine (PS) and phosphatidylethanolamine (PE), toward the cytosolic leaflet of plasma membranes to maintain their asymmetry.[17−20] We adopted a vesicle−plasma membrane fusion method[21−23] to incorporate fluorescent PE (Liss-Rhod-B-PE) into the membrane (Figure S3). When a cell adheres to a glass surface, there is usually a gap between the basal membrane and the surface, which typically varies between 20 and 100 nm depending on the cell type.[24] Therefore, a pseudo total internal reflection (pseudo-TIR) mode[25,26] in which the incident angle is set slightly smaller than the critical angle for TIR was adopted to avoid intensity variation induced by the evanescent field along the z-axis (Figure 2a). Individual fluorophores were tracked and the intensities of the fluorophores were recorded (Figure 2b and Figure S4). In the absence of BD, the fluorescence of the fluorophores was stable (Figure 2c and Figure 2d). The BD solution (5 mM)

https://dx.doi.org/10.1021/acs.nanolett.0c03941
Nano Lett. 2021, 21, 485−491

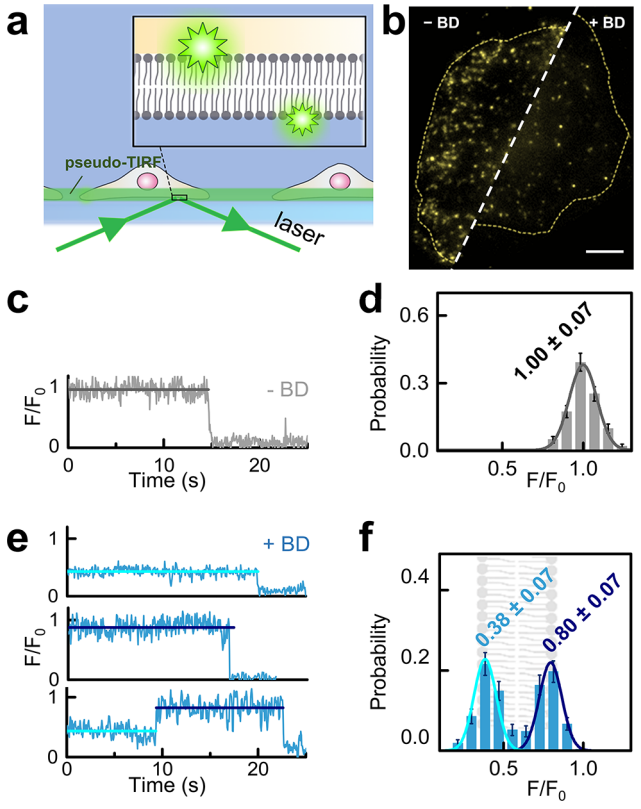

Figure 2. TIRF-based analysis of lipid molecules in the inner/outer leaflets of the cell membrane. (a) Scheme of the pseudo-TIRF illumination on adherent cells. (b) Images of the basal membranes containing Liss-Rhod-B-PE in the absence (left) and presence (right) of BD. Scale bar in the image is 10 μm. (c) Typical fluorescence trace and (d) the corresponding intensity histogram of Liss-Rhod-B-PE in the absence of the quenchers. (e) Typical fluorescence trace and (f) the corresponding intensity histogram of Liss-Rhod-B-PE in the presence of 5 mM BD in the culture medium. Cyan and dark cyan traces and histograms represent lipid molecules at the extracellular and the intracellular surfaces, respectively. Statistics were from 85 traces of 12 cells. Error bars on the histograms represent the statistical error in the bins.

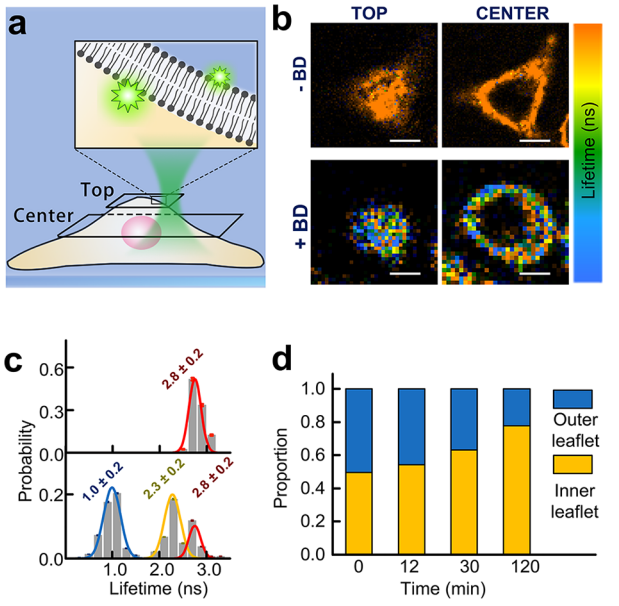

Figure 3. Confocal-based analysis of lipid molecules in the cell membrane. (a) Scheme of the confocal-based FLIM imaging. (b) FLIM images of the top (left) and the midplane (right) of the cell in (a). The two upper panels are images in the absence of the quenchers. The two lower panels are images in the presence of 5 mM BD in the culture medium. Scale bar in the image is 10 μm. (c) Lifetime histograms of the fluorophores in (b) in the absence (upper panel) and presence (lower panel) of the quenchers. (d) Proportions of the Liss-Rhod-B-PE molecules in the outer leaflet (blue) and inner leaflet (yellow) according to the time-lapse imaging of the cells. The histograms were built from data of 16 cells.

percolated into the gap to quench the fluorophores in the membrane. Because the fluorophores in the two opposite surfaces of the lipid bilayer have different distances to the quencher solution, they displayed two relative fluorescent intensities (Figure 2e, f) with F/F_0 = 0.38 ± 0.07 (mean ± s.d.) for the outer surface (cyan) and 0.80 ± 0.07 for the inner surface (dark cyan), where F_0 was the intrinsic fluorescence in the absence of the quenchers (Figure 2d). The centers of the two peaks represent a difference in the distance by 5.2 ± 0.9 nm in consistence with the thickness of the plasma membrane,[8,27,28] indicating that the queenFRET is precise enough to measure the location of a single fluorophore in plasma membranes. Interestingly, besides the traces that displayed low or high intensities, we also observed many traces that illustrated flipping of the fluorophore-labeled PE from the outer leaflet (with low intensity) to the inner leaflet (with high intensity). To the best of our knowledge, this is the first observation of single lipid molecules flipping in live cell membranes.

The positions of the fluorophores in the membrane can also be deduced from their fluorescence lifetimes measured with FLIM by using a time-correlated single photon counting (TCSPC) system (Figure 3a, b). Single molecules cannot be readily imaged in this mode. However, the lifetimes of the fluorophores in a pixel (with a 1 ms dwelling time) can be deduced by fitting the exponentially decaying curve (the TCSPC curve), provided that the fluorophores are sparse enough so that there are less than two fluorophores in each pixel on average (see details in the Supporting Information). The lifetime images of the plasma membranes looked differently in the absence and presence of BD (Figure 3b). We divided the images into small units and calculated the lifetime of each unit to obtain lifetime histograms (see Figure S5 and details in the Supporting Information). The histogram of the intrinsic lifetimes of Liss-Rhod-B attached to PE displayed a peak at 2.8 ± 0.2 ns (Figure 3c, upper panel). When BD solution (5 mM) was added to the Petri dish mounted on the microscope, two additional lifetimes were observed, i.e., 1.0 ± 0.2 ns for the outer surface and 2.3 ± 0.2 ns for the inner surface (Figure 3c, lower panel). We then adopted time-lapse imaging to follow the transmembrane transport of the lipids in Figure 3d. A large proportion of the Liss-Rhod-B-PE molecules were transferred to the inner leaflet when the fluorescent lipids had been incorporated into the membrane for about 120 min. In contrast, no change was observed for the phosphatidylcholine (PC) lipids (Figure S6).

Interaction of Extracellular Proteins with Plasma Membranes. We next demonstrated that queenFRET can monitor interactions of extracellular proteins with plasma membranes. We labeled the human host defense peptide LL-37 with tetramethylrhodamine (TAMRA) at its N-terminus (TAMRA-LL-37) and added the peptide to the culture medium to monitor its membrane insertion dynamics in the lung epithelial carcinoma cell line A549 (Figure 4). LL-37 is a

https://dx.doi.org/10.1021/acs.nanolett.0c03941
Nano Lett. 2021, 21, 485−491

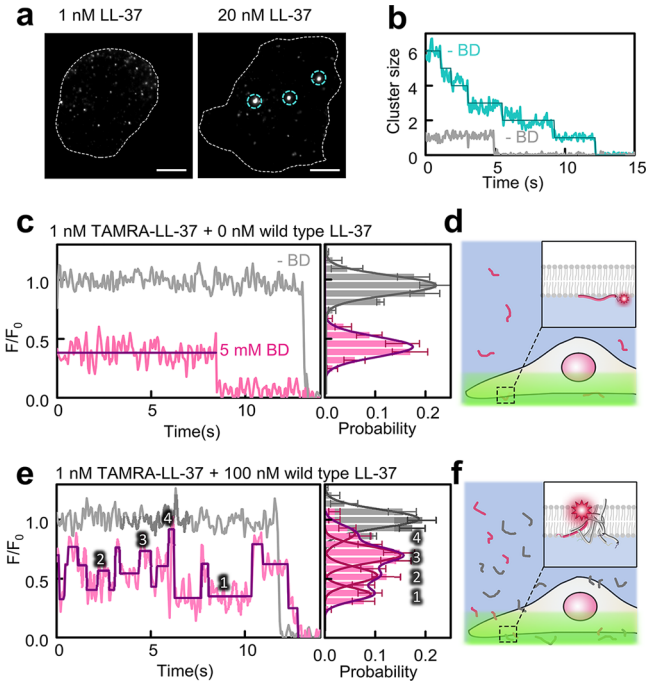

Figure 4. Interaction of the extracellular LL-37 proteins with plasma membranes. (a) Pseudo-TIRF images of N-TAMRA-LL-37 at the plasma membranes at low (left) and high (right) concentrations. LL-37 forms clusters at high concentrations as indicated by the cyan cycles. (b) Photobleaching of an LL-37 monomer (gray) and an LL-37 cluster (cyan) in (a). Scale bar in the image is 10 μm. (c) Typical single molecule fluorescence traces of LL-37 at low concentrations and the corresponding intensity histogram. (d) Scheme of LL-37 at the inner surface of the plasma membrane. (e) Typical single molecule fluorescence traces of LL-37 at high concentrations and the corresponding intensity histogram. (f) Schemes of LL-37 inside the plasma membrane. Gray data were acquired in the absence of the quenchers. Statistics were from 110 traces of 35 cells.

positively charged cathelicidin that targets negatively charged bacterial membranes.[29] It also binds cancer cells with exposed anionic lipids.[30] Upon incubation, the peptide percolated into the thin gap between the basal membrane and the glass surface, where it interacted with the plasma membranes (Figure 4a). After illuminating the sample for 30 s to bleach a large fraction of the TAMRA-LL-37 molecules, individual fluorescence spots were observed to diffuse on the basal membrane. At a low protein concentration (1 nM), LL-37 usually maintains as monomers, and typical intensity traces showed a single photobleaching step (Figure 4a, left panel; Figure 4b, gray trace). At higher protein concentrations, for example, at 20 nM LL-37, some bright fluorescence spots could be observed (Figure 4a, right panel). Typical intensity traces of these spots displayed multiple photobleaching steps, indicating that LL-37 formed oligomers at higher concentrations (Figure 4b, cyan trace). Figure 4c illustrates the comparison of the monomeric TAMRA-LL-37 (1 nM) in the absence (gray) and presence (pink) of 5 mM BD. Both intensity traces are stable. The ratio of the fluorescent intensities, F/F_0, is in agreement with the calculation assuming that the monomeric TAMRA-LL-37 adsorbed and laid on the surface of the A549 cell (Figure 4d). At an elevated concentration (1 nM TAMRA-LL-37 mixed with 100 nM wild type LL-37), LL-37 became dynamic, switching between different depths (Figure 4e). While the intensity of TAMRA-LL-37 remained stable in the absence of BD (gray), the intensity histogram of the dynamic TAMRA-LL-37 displayed three major peaks in the presence of BD (pink). The peaks can be converted to insertion depths of 0.1 ± 0.9, 2.1 ± 0.9, and 4.7 ± 0.9 nm (Figure 4e). The fourth peak with the highest intensity could be attributed to fluorophores near the intracellular surface, which could not be accurately positioned because they were in the insensitive region of our approach (see Figure S7 and details in the Supporting Information). The results were similar to those obtained from our previously developed in vitro methods,[31] again demonstrating the validity of queenFRET. The results suggest that LL-37 forms oligomers and displays dynamic behavior in live cell membranes, possibly associated with the mechanism of its anticancer functions.[30]

Interaction of Intracellular Proteins with Plasma Membranes. We finally investigated the insertion of proteins from the intracellular side of cell membranes, which is valuable when endogenous proteins are of interest. Conventional techniques were only able to tell us whether a protein of interest is at the membrane or not. QueenFRET can distinguish not only different membrane-inserting proteins but also different insertion states of the same protein in the membrane. For simplicity, we delivered purified proteins into the cells to mimic endogenous proteins (Figure S8). The mixed lineage kinase domain-like protein (MLKL) was used as an example, which is crucial for necroptosis by permeabilizing membranes through its N-terminal region upon phosphorylation.[32,33] It was reported that the short form of MLKL (residues 2−123; $MLKL_{2-123}$) is more active than the long form of MLKL (residues 2−154; $MLKL_{2-154}$) which contains a brace helix (19). We labeled $MLKL_{2-123}$ and $MLKL_{2-154}$ at the residue S55 with TAMRA and delivered them into the human monocytic-like cell line THP-1 (Figure S8). The cells were then suspended in a microfluidic channel and imaged by FLIM (Figure 5a). The lifetime histogram for $MLKL_{2-154}$ indicated that they inserted into the membrane shallowly (peak at 2.4 ns in Figure 5b). In contrast, $MLKL_{2-123}$ might insert into the membrane more deeply at 2.7 nm (1.9 ns peak) and 4.6 nm (1.4 ns peak) (Figure 5c). The extra peak (red fitting curve) represent molecules in the cytoplasm. Our results are qualitatively consistent with previous reports,[34] but queenFRET provides a much more quantitative description. The observation that $MLKL_{2-123}$ inserts into the membrane in three different depths is very interesting. It suggests that the protein may change conformations upon interaction with the membrane, a phenomenon that deserves deeper investigation in the future.

Probing the structural dynamics of biomolecules in plasma membranes had been a very difficult task. Here, we demonstrated the feasibility of queenFRET in quantitating transmembrane trafficking of a fluorophore-labeled biomolecule from not only the inside but also the outside of living cells. Both locations are crucial to understanding protein−membrane and protein−ligand interactions. Our method is especially useful when the biomolecules of interest interact with the cytosolic leaflet of the plasma membrane, which is not accessible by conventional techniques at the single molecular level. QueenFRET can be implemented with both TIRFM and FLIM. The prerequisite is to label the molecules of interest with small fluorophores. TIRFM is preferred when investigating the dynamics of plasma membranes adhered to glass surfaces. Confocal-based FLIM is a good choice to observe floating cells such as those in microfluidic channels or even inside a cluster of cells.

https://dx.doi.org/10.1021/acs.nanolett.0c03941
Nano Lett. 2021, 21, 485−491

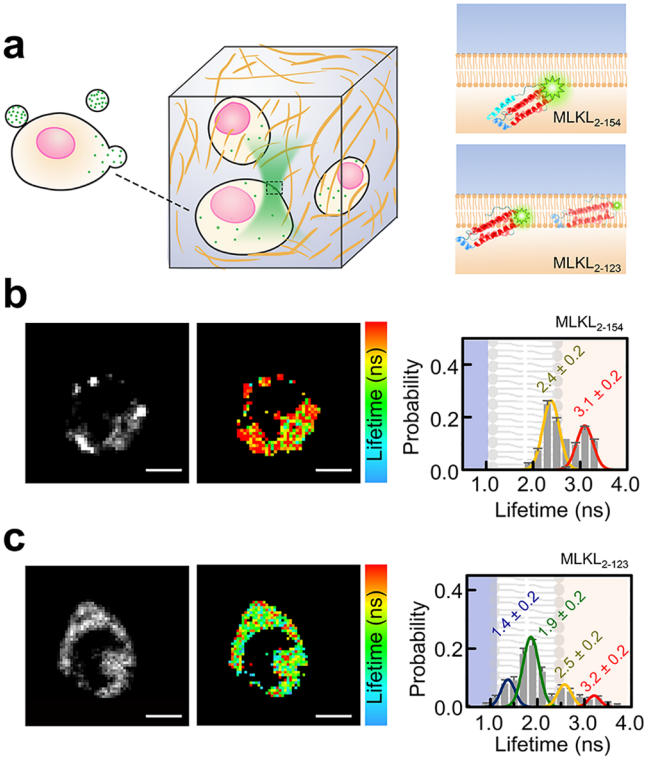

Figure 5. Interaction of the intracellular MLKL proteins with plasma membranes. (a) Scheme of MLKL in the THP-1 cells suspended in a microchip for confocal-based FLIM. (b) Intensity image (left), lifetime map (middle), and lifetime histogram (right) of TARMA-labeled $MLKL_{2-154}$. (c) Data for TARMA-labeled $MLKL_{2-123}$. Color bar is from 1.5 to 3.0 ns. Scale bar = 5 μm. The concentration of BD was 5 mM. The histograms were built from data of 10 cells.

Choosing appropriate quenchers and donors is crucial to perform the queenFRET successfully. The quenchers should fulfill the following requirements. (1) They should have sufficient solubility. According to our calculations (Figure 1b), the concentration of the extracellular quenchers should be as high as a few millimoles per liter to produce sufficient FRET with the donors. (2) They should exhibit appropriate spectral properties. The quenchers, which serve as the FRET acceptors, should have a high extinction coefficient. In addition, the absorption spectrum of the quencher should show significant overlap with the emission spectrum of the donors, allowing effective energy transfer even at relatively large donor−quencher distances so that the positional changes of the donor near the cytosolic surface of the cell membrane can be readily observed. (3) They should have low fluorescence emission. The quenchers should be nonfluorescent (at least of low emission at the detection window of the donors) in order to not interfere with the fluorescent signals of the donors. Moreover, as in other in vivo measurements, additional requests on the quenchers should be satisfied. (1) Nontoxicity should be satisfied. Biocompatibility is the primary factor to be considered. For example, some dyes may undergo photochemical reactions and cause damage to various biological substrates.[35,36] BD in our work is nontoxic to cells, allowing us to observe biomolecule dynamics for a few hours. (2) Negligible interactions with the cell surface should be satisfied. Plasma membranes are complicated systems that consist of various biomolecules with different physical and chemical properties. Interactions of the plasma membranes with the quenchers may alter their spatial distribution near the membranes, thus changing the dependence of FRET efficiency on the distances and resulting in uncertainty when interpreting the fluorescent signals. Ideal quenchers should not have any interactions with the cell surfaces. Care should also be taken when choosing donors. Fluorophores used to label the biomolecules should avoid strong interactions with the membranes because they may alter the membrane-interacting patterns of the biomolecules of interest.[37] In addition, fluorophores that are sensitive to solvent polarity should also be avoided unless the fluorophores remain in the same environment, for example, always in the membrane during the measurements.[38]

It is noteworthy that the absolute fluorescence intensity is not necessary to gain the positions of the fluorophores in the membranes. In our approach, the distance (d) between the donor and the interface of the quencher solution and the membrane was determined by comparing the measured relative intensity (F/F_0) or relative lifetime (τ/τ_0) with the calculated curves like the ones displayed in Figure 1b. One should first measure the intrinsic parameters F_0 and/or τ_0, which are the F and/or τ under the same conditions as in the actual measurements but without adding the quenchers. These two intrinsic parameters should be used as references in the data analysis. QueenFRET is of subnanometer precision. For example, three theoretical curves for Liss-Rhod-B at three BD concentrations are displayed in Figure S7a. The inverse of the digital differentials of them is displayed in Figure S7b, from which we can estimate the error in distance. The same analysis applies to errors in lifetime measurements.

In the present work, we have focused on the transmembrane positions of fluorophores disregarding their in-plane movements. Our method can work along with many localization-based imaging techniques. For example, the in-plane movements of the biomolecules can be recorded by existing methods such as single-molecule tracking and super-resolution imaging. We anticipate that the combination of queenFRET with super-resolution imaging[39] may significantly improve our understanding of membrane trafficking, receptor responses, and signal transductions of live cells, to name just a few.

■ ASSOCIATED CONTENT

Supporting Information

The Supporting Information is available free of charge at https://pubs.acs.org/doi/10.1021/acs.nanolett.0c03941.

(Note 1) Live cell imaging; (Note 2) distance dependence of the fluorescence signal; (Note 3) lifetime analysis in FLIM; (Note 4) calibration of the Fürster distances (r_0) between one donor and one quencher; (Note 5) optical setups; (Note 6) sample preparation details of experimental materials and methods; absorption spectrum of the Blue Dextran used in our assays (Figure S1), Cell Counting Kit-8 (CCK-8) assay of the viability of A549 cells in the culturing medium with (red) and without (black) BD (Figure S2), incorporation of Liss-Rhod-B-PE into plasma membranes (Figure S3), 3D trace of a lipid molecule and a peptide molecule in the plasma membranes (Figure S4), unit-by-unit analysis of the lifetimes (Figure S5), control experiment with NBD-labeled PC in the plasma membranes (Figure S6), analysis of the resolution (Figure S7), delivery of the MLKL protein into cells (Figure S8), calibration of the Fürster distance (r_0) between Liss-Rhod-B-PE and BD in the

https://dx.doi.org/10.1021/acs.nanolett.0c03941
Nano Lett. 2021, 21, 485−491

Supporting Information (Figure S9); and the amino acid sequences of the LL-37 peptide used in this work (Table 1) (PDF)

AUTHOR INFORMATION

Corresponding Authors

Ming Li − *Beijing National Laboratory for Condensed Matter Physics, Institute of Physics, Chinese Academy of Sciences, Beijing 100190, China; Songshan Lake Materials Laboratory, Dongguan, Guangdong 523808, China; University of Chinese Academy of Sciences, Beijing 100049, China;* orcid.org/0000-0002-5328-5826; Email: mingli@iphy.ac.cn

Ying Lu − *Beijing National Laboratory for Condensed Matter Physics, Institute of Physics, Chinese Academy of Sciences, Beijing 100190, China; Songshan Lake Materials Laboratory, Dongguan, Guangdong 523808, China; University of Chinese Academy of Sciences, Beijing 100049, China;* orcid.org/0000-0002-8421-7228; Email: yinglu@iphy.ac.cn

Authors

Wenqing Hou − *Beijing National Laboratory for Condensed Matter Physics, Institute of Physics, Chinese Academy of Sciences, Beijing 100190, China; Songshan Lake Materials Laboratory, Dongguan, Guangdong 523808, China; University of Chinese Academy of Sciences, Beijing 100049, China*

Dongfei Ma − *Beijing National Laboratory for Condensed Matter Physics, Institute of Physics, Chinese Academy of Sciences, Beijing 100190, China; Songshan Lake Materials Laboratory, Dongguan, Guangdong 523808, China*

Xiaolong He − *Beijing National Laboratory for Condensed Matter Physics, Institute of Physics, Chinese Academy of Sciences, Beijing 100190, China*

Weijing Han − *Songshan Lake Materials Laboratory, Dongguan, Guangdong 523808, China*

Jianbing Ma − *Beijing National Laboratory for Condensed Matter Physics, Institute of Physics, Chinese Academy of Sciences, Beijing 100190, China; Songshan Lake Materials Laboratory, Dongguan, Guangdong 523808, China*

Hao Wang − *Beijing National Laboratory for Condensed Matter Physics, Institute of Physics, Chinese Academy of Sciences, Beijing 100190, China; Songshan Lake Materials Laboratory, Dongguan, Guangdong 523808, China; University of Chinese Academy of Sciences, Beijing 100049, China*

Chunhua Xu − *Beijing National Laboratory for Condensed Matter Physics, Institute of Physics, Chinese Academy of Sciences, Beijing 100190, China*

Ruipei Xie − *Beijing National Laboratory for Condensed Matter Physics, Institute of Physics, Chinese Academy of Sciences, Beijing 100190, China; University of Chinese Academy of Sciences, Beijing 100049, China*

Qihui Fan − *Beijing National Laboratory for Condensed Matter Physics, Institute of Physics, Chinese Academy of Sciences, Beijing 100190, China*

Fangfu Ye − *Beijing National Laboratory for Condensed Matter Physics, Institute of Physics, Chinese Academy of Sciences, Beijing 100190, China; Songshan Lake Materials Laboratory, Dongguan, Guangdong 523808, China; University of Chinese Academy of Sciences, Beijing 100049, China*

Shuxin Hu − *Beijing National Laboratory for Condensed Matter Physics, Institute of Physics, Chinese Academy of Sciences, Beijing 100190, China*

Complete contact information is available at: https://pubs.acs.org/10.1021/acs.nanolett.0c03941

Author Contributions

M.L. and Y.L. designed the study. W.Q.H., D.F.M., X.L.H., and C.H.X. performed the experiments. X.L.H. and S.X.H. prepared proteins. R.P.X., Q.H.F., and F.F.Y. prepared microfluidic channels. W.Q.H., D.F.M., M.L., Y.L., J.B.M., H.W., and W.J.H. analyzed the data. M.L., Y.L., and W.Q.H. wrote the manuscript.

Author Contributions

‖W.Q.H., D.F.M., and X.L.H. contributed equally to this work.

Notes

The authors declare no competing financial interest.

ACKNOWLEDGMENTS

This work was supported by the National Key Research and Development program of China (2019YFA0709304), the National Natural Science Foundation of China (11974411 to Y.L. and 91753104 to M.L.), the Outstanding Young Scholars of the National Natural Science Foundation of China (12022409 to Y.L.), the CAS Key Research Program of Frontier Sciences (QYZDJ-SSW-SYS014 to M.L. and ZDBS-LY-SLH015 to Y.L.), and the CAS Youth Innovation Promotion Association (2017015 to Y.L.). The authors also gratefully acknowledge the support of the K. C. Wong Education Foundation.

REFERENCES

(1) Bretscher, M. S.; Raff, M. C. Mammalian plasma membranes. *Nature* **1975**, *258* (5530), 43−9.

(2) Leth-Larsen, R.; Lund, R. R.; Ditzel, H. J. Plasma membrane proteomics and its application in clinical cancer biomarker discovery. *Mol. Cell. Proteomics* **2010**, *9* (7), 1369−82.

(3) Contreras, F. X.; Sanchez-Magraner, L.; Alonso, A.; Goni, F. M. Transbilayer (flip-flop) lipid motion and lipid scrambling in membranes. *FEBS Lett.* **2010**, *584* (9), 1779−86.

(4) Nishida, N.; Osawa, M.; Takeuchi, K.; Imai, S.; Stampoulis, P.; Kofuku, Y.; Ueda, T.; Shimada, I. Functional dynamics of cell surface membrane proteins. *J. Magn. Reson.* **2014**, *241*, 86−96.

(5) Radic, M.; Pattanaik, D. Cellular and Molecular Mechanisms of Anti-Phospholipid Syndrome. *Front. Immunol.* **2018**, *9*, 969.

(6) Naito, A.; Matsumori, N.; Ramamoorthy, A. Dynamic membrane interactions of antibacterial and antifungal biomolecules, and amyloid peptides, revealed by solid-state NMR spectroscopy. *Biochim. Biophys. Acta, Gen. Subj.* **2018**, *1862* (2), 307−323.

(7) Nicolson, G. L. Cell membrane fluid-mosaic structure and cancer metastasis. *Cancer Res.* **2015**, *75* (7), 1169−76.

(8) Engelman, D. M. Membranes are more mosaic than fluid. *Nature* **2005**, *438* (7068), 578−80.

(9) Halls, M. L.; Canals, M. Genetically Encoded FRET Biosensors to Illuminate Compartmentalised GPCR Signalling. *Trends Pharmacol. Sci.* **2018**, *39* (2), 148−157.

(10) Roy, R.; Hohng, S.; Ha, T. A practical guide to single-molecule FRET. *Nat. Methods* **2008**, *5* (6), 507−16.

(11) Weiss, S. Fluorescence spectroscopy of single biomolecules. *Science* **1999**, *283* (5408), 1676−1683.

(12) Michalet, X.; Weiss, S.; Jager, M. Single-molecule fluorescence studies of protein folding and conformational dynamics. *Chem. Rev.* **2006**, *106* (5), 1785−1813.

(13) Lee, J.; Lee, S.; Ragunathan, K.; Joo, C.; Ha, T.; Hohng, S. Single-Molecule Four-Color FRET. *Angew. Chem., Int. Ed.* **2010**, *49* (51), 9922−9925.

(14) Ma, D. F.; Xu, C. H.; Hou, W. Q.; Zhao, C. Y.; Ma, J. B.; Huang, X. Y.; Jia, Q.; Ma, L.; Diao, J.; Liu, C.; Li, M.; Lu, Y. Detecting Single-Molecule Dynamics on Lipid Membranes with Quenchers-in-a-Liposome FRET. *Angew. Chem., Int. Ed.* **2019**, *58* (17), 5577−5581.

(15) Thompson, S. T.; Stellwagen, E. Binding of Cibacron blue F3GA to proteins containing the dinucleotide fold. *Proc. Natl. Acad. Sci. U. S. A.* **1976**, *73* (2), 361−5.
(16) Thompson, S. T.; Cass, K. H.; Stellwagen, E. Blue dextran-sepharose: an affinity column for the dinucleotide fold in proteins. *Proc. Natl. Acad. Sci. U. S. A.* **1975**, *72* (2), 669−72.
(17) Kobayashi, T.; Menon, A. K. Transbilayer lipid asymmetry. *Curr. Biol.* **2018**, *28* (8), R386−R391.
(18) Holthuis, J. C. M.; van Meer, G.; Huitema, K. Lipid microdomains, lipid translocation and the organization of intracellular membrane transport (Review). *Mol. Membr. Biol.* **2003**, *20* (3), 231−241.
(19) Tang, X.; Halleck, M. S.; Schlegel, R. A.; Williamson, P. A subfamily of P-type ATPases with aminophospholipid transporting activity. *Science* **1996**, *272* (5267), 1495−7.
(20) van Meer, G.; Voelker, D. R.; Feigenson, G. W. Membrane lipids: where they are and how they behave. *Nat. Rev. Mol. Cell Biol.* **2008**, *9* (2), 112−24.
(21) Tanaka, Y.; Schroit, A. J. Insertion of Fluorescent Phosphatidylserine into the Plasma-Membrane of Red-Blood-Cells - Recognition by Autologous Macrophages. *J. Biol. Chem.* **1983**, *258* (18), 1335−1343.
(22) McIntyre, J. C.; Sleight, R. G. Fluorescence assay for phospholipid membrane asymmetry. *Biochemistry* **1991**, *30* (51), 11819−27.
(23) Kleusch, C.; Hersch, N.; Hoffmann, B.; Merkel, R.; Csiszar, A. Fluorescent lipids: functional parts of fusogenic liposomes and tools for cell membrane labeling and visualization. *Molecules* **2012**, *17* (1), 1055−73.
(24) Chizhik, A. I.; Rother, J.; Gregor, I.; Janshoff, A.; Enderlein, J. Metal-induced energy transfer for live cell nanoscopy. *Nat. Photonics* **2014**, *8* (2), 124−127.
(25) Wang, D.; Agrawal, A.; Piestun, R.; Schwartz, D. K. Enhanced information content for three-dimensional localization and tracking using the double-helix point spread function with variable-angle illumination epifluorescence microscopy. *Appl. Phys. Lett.* **2017**, *110* (21), 211107.
(26) Kapanidis, A. N.; Weiss, S. Fluorescent probes and bioconjugation chemistries for single-molecule fluorescence analysis of biomolecules. *J. Chem. Phys.* **2002**, *117* (24), 10953−10964.
(27) Nagle, J. F.; Tristram-Nagle, S. Structure of lipid bilayers. *Biochim. Biophys. Acta, Rev. Biomembr.* **2000**, *1469* (3), 159−95.
(28) Cybulski, L. E.; de Mendoza, D. Bilayer Hydrophobic Thickness and Integral Membrane Protein Function. *Curr. Protein Pept. Sci.* **2011**, *12* (8), 760−766.
(29) Xhindoli, D.; Pacor, S.; Benincasa, M.; Scocchi, M.; Gennaro, R.; Tossi, A. The human cathelicidin LL-37−A pore-forming antibacterial peptide and host-cell modulator. *Biochim. Biophys. Acta, Biomembr.* **2016**, *1858* (3), 546−66.
(30) Wu, W. K.; Wang, G.; Coffelt, S. B.; Betancourt, A. M.; Lee, C. W.; Fan, D.; Wu, K.; Yu, J.; Sung, J. J.; Cho, C. H. Emerging roles of the host defense peptide LL-37 in human cancer and its potential therapeutic applications. *Int. J. Cancer* **2010**, *127* (8), 1741−7.
(31) Li, Y.; Qian, Z.; Ma, L.; Hu, S.; Nong, D.; Xu, C.; Ye, F.; Lu, Y.; Wei, G.; Li, M. Single-molecule visualization of dynamic transitions of pore-forming peptides among multiple transmembrane positions. *Nat. Commun.* **2016**, *7*, 12906.
(32) Gong, Y.; Fan, Z.; Luo, G.; Yang, C.; Huang, Q.; Fan, K.; Cheng, H.; Jin, K.; Ni, Q.; Yu, X.; Liu, C. The role of necroptosis in cancer biology and therapy. *Mol. Cancer* **2019**, *18* (1), 100.
(33) Petrie, E. J.; Czabotar, P. E.; Murphy, J. M. The Structural Basis of Necroptotic Cell Death Signaling. *Trends Biochem. Sci.* **2019**, *44* (1), 53−63.
(34) Su, L.; Quade, B.; Wang, H.; Sun, L.; Wang, X.; Rizo, J. A plug release mechanism for membrane permeation by MLKL. *Structure* **2014**, *22* (10), 1489−500.
(35) Caetano, W.; Haddad, P. S.; Itri, R.; Severino, D.; Vieira, V. C.; Baptista, M. S.; Schroder, A. P.; Marques, C. M. Photo-induced destruction of giant vesicles in methylene blue solutions. *Langmuir* **2007**, *23* (3), 1307−14.
(36) Tuite, E. M.; Kelly, J. M. Photochemical interactions of methylene blue and analogues with DNA and other biological substrates. *J. Photochem. Photobiol., B* **1993**, *21* (2−3), 103−24.
(37) Hughes, L. D.; Rawle, R. J.; Boxer, S. G. Choose your label wisely: water-soluble fluorophores often interact with lipid bilayers. *PLoS One* **2014**, *9* (2), No. e87649.
(38) Ladokhin, A. S.; Selsted, M. E.; White, S. H. Bilayer interactions of indolicidin, a small antimicrobial peptide rich in tryptophan, proline, and basic amino acids. *Biophys. J.* **1997**, *72* (2), 794−805.
(39) Chen, Q. X.; Shao, X. T.; Hao, M. G.; Fang, H. B.; Guan, R. L.; Tian, Z. Q.; Li, M. L.; Wang, C. R.; Ji, L. N.; Chao, H.; Guan, J. L.; Diao, J. J. Quantitative analysis of interactive behavior of mitochondria and lysosomes using structured illumination microscopy. *Biomaterials* **2020**, *250*, 120059.

https://dx.doi.org/10.1021/acs.nanolett.0c03941
Nano Lett. 2021, 21, 485−491